Extremely high-frequency self-pulsations in chirped-grating distributed-feedback semiconductor lasers

Yuan-Hwang Liao and Herbert G. Winful
Department of Electrical Engineering and Computer Science, University of Michigan, 1301 Beal Avenue, Ann Arbor, Michigan 48109-2122

(Received 31 July 1996; accepted for publication 20 August 1996)

We show that an asymmetrically chirped, single-section distributed-feedback (DFB) laser is capable of sustained self-pulsations at frequencies in excess of 200 GHz. These pulsations arise from mode beating and are absent in uniform or symmetrically chirped DFB lasers. For sufficiently large coupling constants, the pulsation frequency can approach a terahertz. © *1996 American Institute of Physics.* [S0003-6951(96)02344-3]

In this letter we present a large signal analysis of the dynamics of chirped-grating distributed-feedback (CG-DFB) semiconductor lasers. Our results show that an asymmetrically chirped, single-section DFB laser can undergo sustained self-pulsations at frequencies in excess of 200 GHz. These pulsations result from the beating between two asymmetric longitudinal modes with different frequencies but similar gains. The carrier population distribution remains essentially frozen during these pulsations and, hence, can be adiabatically eliminated. For first order gratings an asymmetric chirp profile is necessary for the observation of these ultrahigh frequency pulsations. Uniform or symmetrically chirped DFB lasers do not exhibit this instability at the power levels considered here.

Chirped-grating DFB lasers are of interest because of their potential for true single mode operation and their resistance to longitudinal spatial hole burning.[1–3] Also of great current interest are self-pulsating DFB lasers that pulsate at multigigahertz frequencies.[4–7] Applications of these high-frequency self-pulsating lasers include clock recovery in optical communications systems.[6] The mechanisms for high-frequency self-pulsations are thought to be unique to multisection DFB lasers and are classified as either dispersive Q-switching or mode beating oscillations.[7] Here we show that these high-frequency oscillations can also occur in simpler single-section DFB lasers with the appropriate chirp.

A schematic of the chirped DFB laser structure is shown in Fig. 1 for both symmetric and asymmetric chirp. For a linearly chirped grating the z-dependent pitch can be expressed as

$$\Lambda(z)=\Lambda_0+\eta\Lambda_0^2 z, \tag{1}$$

for an asymmetrically chirped grating. Here Λ_0 is the reference grating pitch at the cavity center ($z=0$) and η is the chirp factor. Within the laser, the total field is taken as a sum of forward and backward propagating waves

$$E=E_F(z,t)\exp[i(\beta_0 z-\omega t)]+E_B(z,t)\times\exp(-i(\beta_0 z+\omega t)], \tag{2}$$

where $\beta_0=\pi/\Lambda_0$ is the reference wave number. The slowly varying amplitudes of the forward (E_F) and backward (E_B) waves satisfy the propagation equations

$$\frac{1}{v_g}\frac{\partial E_F}{\partial t}+\frac{\partial E_F}{\partial z}=i\kappa E_B\exp(-i\eta z^2)+\left[\frac{\Gamma g(N)}{2}-\alpha_s-i\Delta\beta(N)\right]E_F, \tag{3}$$

$$\frac{1}{v_g}\frac{\partial E_B}{\partial t}-\frac{\partial E_B}{\partial z}=i\kappa E_F\exp(i\eta z^2)+\left[\frac{\Gamma g(N)}{2}-\alpha_s-i\Delta\beta(N)\right]E_B, \tag{4}$$

which are coupled to the carrier density (N) rate equation

$$\frac{dN}{dt}=\frac{J}{ed}-\gamma N-v_g g(|E_F|^2+|E_B|^2). \tag{5}$$

In these equations, v_g is the group velocity of light in the active medium, κ is the grating coupling coefficient, Γ is the mode confinement factor, g is the gain, α_s is the loss due to absorption and scattering, and $\Delta\beta$ is a carrier–density dependent detuning from Bragg condition at cavity center. In Eq. (5) J is the injection current density, d is the active layer thickness, and e is the charge of the electron. The recombination rate is

$$\gamma=1/\tau+BN+CN^2, \tag{6}$$

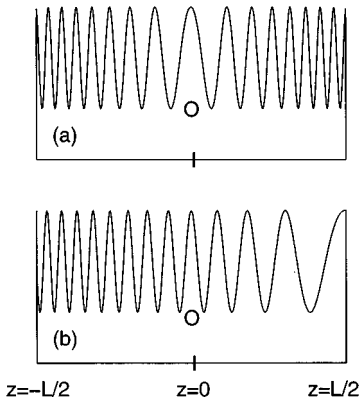

FIG. 1. A schematic of the chirped-grating DFB laser structure with (a) symmetric and (b) asymmetric chirp.

TABLE I. Typical parameter values used in simulation.

Linear carrier lifetime (τ)	4 ns
Bimolecular recombination coefficient (B)	1×10^{-10} cm^3 s^{-1}
Auger recombination coefficient (C)	3×10^{-29} cm^6 s^{-1}
Differential gain (a)	3×10^{-16} cm^2
Transparency carrier density (N_0)	1.5×10^{18} cm^{-3}
Absorption and scattering loss (α_s)	40 cm^{-1}
Active layer thickness (d)	0.18 μm
Approximate emission wavelength (λ_0)	1.55 μm
Effective refractive index (n_{eff})	3.7
Confinement factor (Γ)	0.35
Gain suppression coefficient (ϵ)	1×10^{-17} cm^3

with τ being the linear recombination lifetime, B the bimolecular recombination coefficient, and C the Auger recombination coefficient.

The dependence of the gain on carrier density is described by

$$g=[a(N-N_0)]/(1+\epsilon S), \tag{7}$$

where a is the differential gain, N_0 is the carrier density at transparency, ϵ is the gain compression coefficient, and $S=|E_F|^2+|E_B|^2$. The detuning is given by

$$\Delta\beta(N)=[-\Gamma a\alpha_H(N-N_0)]/2, \tag{8}$$

where α_H is the linewidth enhancement factor. In our simulations we find that the change in detuning due to carrier density variations is much smaller than the externally imposed grating chirp and, hence, can be neglected.

Equations (3)–(5) are solved subject to the boundary conditions $E_B(L/2,t)=E_F(-L/2,t)=0$, where $L=400$ μm is the cavity length.[8,9] Typical parameter values used in the simulation are quoted in Table I. For small values of the chirp factor ($C\equiv\eta L^2<1$) our simulations yield the well known static properties of CG-DFB lasers.[1,2] (Note that $C=1$ corresponds to a change in pitch of about 0.05%.) For uniform index-coupled DFB lasers, there are two lowest order modes ($+1$ and -1) of equal threshold gain that are symmetrically disposed on either side of the Bragg frequency. This degeneracy in threshold gains persists in the presence of an asymmetric linear chirp. It takes a symmetric grating chirp to lift this degeneracy and improve axial mode selectivity.

We first consider an antisymmetric linear chirp of the form depicted in Fig. 1(b) and described by Eq. (1). Figure 2 shows the temporal evolution of the output from the left ($z=-L/2$) and right ($z=L/2$) ends of the laser when operating in the low frequency -1 mode with $\kappa L=2.0$, $C=0.5$, and pump current $I=200$ mA. The output power from the two ends is asymmetric and this asymmetry increases with pump current and chirp factor. The inset in Fig. 2 shows the photon density profiles of the -1 (solid curve) and $+1$ modes in steady state. The two different modes are excited by changing the initial conditions.

For the same coupling constant ($\kappa L=2.0$) and pump current ($I=200$ mA), these degenerate modes become unstable for large values of the chirp factor. Figure 3(a) shows the temporal evolution of the output power for a chirp factor $C=2.0$. The output exhibits sustained pulsations after the initial transient relaxation oscillations. As shown in the inset,

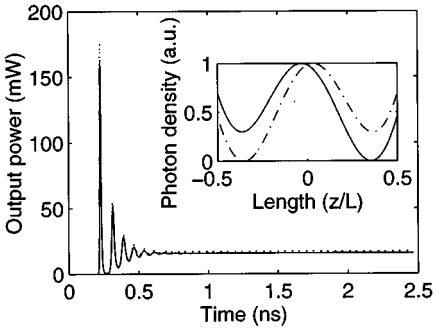

FIG. 2. The temporal evolution of the output from the left ($z=-L/2$, dotted curve) and right ($z=L/2$, solid curve) ends of the laser when operating in -1 mode with $\kappa L=2.0$, $C=0.5$, and $I=200$ mA. The inset shows the photon density profiles of the -1 (solid curve) and $+1$ (dash-dotted curve) modes in steady state.

the pulsations from the opposite ends of the laser are in antiphase and have a frequency of 212.5 GHz. The modulation depth is close to 100% around an average value of 17 mW. Figure 3(b) shows the spatiotemporal evolution of the cavity photon density. The longitudinal field distribution appears to oscillate between the two asymmetric modes. This suggests that the observed pulsations in the output result from beating between these two modes. To test this hypothesis, we calculate the frequency separation between the $+1$ and -1 modes from

$$\Delta\nu=\frac{(\Delta\beta L)c}{\pi n_{\text{eff}}L}, \tag{9}$$

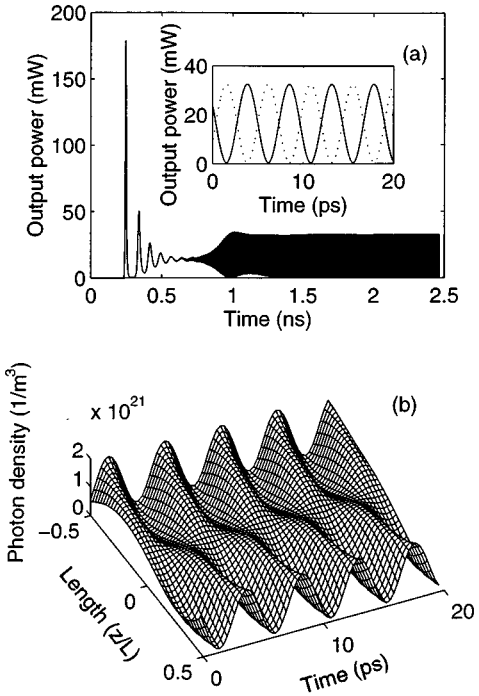

FIG. 3. (a) The temporal evolution of the output power from the right end ($z=L/2$) with $\kappa L=2.0$, $C=2.0$, and $I=200$ mA. The inset shows the time evolution from both the left (dotted curve) and right (solid curve) ends in the last 20 ps. (b) The spatiotemporal evolution of the cavity photon density in the last 20 ps.

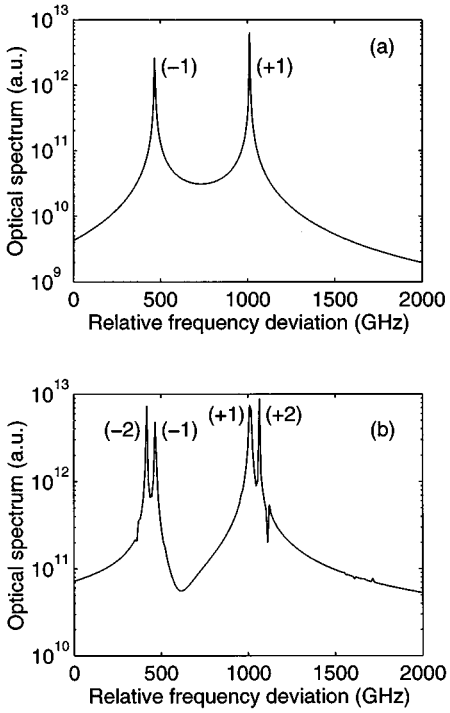

FIG. 4. (a) The optical spectrum of the output from the right end of the laser with $\kappa L=8.0$, $C=2.0$, and $I=90$ mA. The two lines corresponding to the $+1$ and -1 mode are separated by 550 GHz. (b) The optical spectrum of $\kappa L=8.0$, $C=2.0$, and $I=400$ mA with $+2$ and -2 additional modes.

where $\Delta\beta L$ is determined from steady-state threshold conditions.[10] For $\kappa L=2.0$ we find $\Delta\beta L=3.3$, which yields a frequency separation of 212.9 GHz. This agrees with the observed pulsation frequency of 212.5 GHz, thus, confirming the hypothesis that the oscillations are the beat note between the two asymmetric modes.

If the pulsations result from the beating between two modes with similar gains, it should be possible to increase the pulsation frequency by increasing the frequency splitting of the two modes. This can be easily achieved by increasing the coupling constant κ. Noting that DFB lasers with coupling constants as high as $\kappa=300$ cm^{-1} have been demonstrated,[5] we conservatively take $\kappa=200$ cm^{-1}, $\kappa L=8.0$ for a 400-μm-long device. Once again, a steady-state threshold calculation yields $\Delta\beta L=8.5$, which when used in Eq. (9) results in a frequency splitting between the two modes of $\Delta\nu=550$ GHz. A simulation of Eqs. (3)–(5) with $\kappa L=8.0$, $I=90$ mA, and $C=2.0$ yields a pulsation frequency of 550 GHz in agreement with the predicted value. Figure 4(a) shows the calculated optical spectrum of the output from the right end of the laser. We observe two lines corresponding to the $+1$ and -1 mode separated by 550 GHz. The asymmetry in the spectrum is due to the fact that the $+1$ mode has higher power at the right end than the -1 mode does. (At the left end the asymmetry in spectral power is reversed.) For much higher pump currents, the output pulsations become quasiperiodic as higher order modes are excited. The spectrum shown in Fig. 4(b) for $I=400$ mA, now reveals two additional modes, the $+2$ and -2 modes together with the lowest order modes.

An important feature of these high-frequency oscillations is that the carrier–density distribution remains essentially frozen while the field undergoes large-amplitude excursions. We observe a tiny ripple in the carrier density at the beat frequency due to the nonlinear interaction with the two longitudinal modes. This ripple is so small that the carrier density can be adiabatically eliminated and the dynamics described more simply by the two coupled field equations. Numerical solutions of the coupled field equations yield the same multi-100 GHz oscillations displayed by the full set of coupled field and carrier equations.

A deeper understanding of these high-frequency oscillations may be gained by considering the analysis of Wenzel *et al.*[7] of fast self-pulsations in two-section DFB lasers. Wenzel *et al.* showed that beating-type oscillations can occur in two-section DFB lasers if the two sections are detuned from each other. The beats occur between two instantaneous modes of the composite structure that have identical threshold gains but different longitudinal spatial profiles. Our single section, asymmetric, linearly chirped DFB laser can be thought of as a ''two-section'' device: a high-frequency grating section ($\Lambda(z)<\Lambda_0$) at the left end and a low-frequency grating section ($\Lambda(z)>\Lambda_0$) at the right end. The left side acts as a DFB laser for the $+1$ mode while the right side acts as an amplifier for the same mode. The role of amplifier and laser are reversed for the -1 mode. The mutual injection by these two detuned laser sections will produce beat oscillations when the detuning lies outside a certain locking range. The need for a detuning implies that a chirped, single-section device will not exhibit these high-frequency pulsations if the chirp is symmetric about the midpoint. In that case, the two subsections have equal frequencies and, hence, no beat oscillations will occur. We have confirmed this with a solution of Eqs. (3)–(5) for a symmetrically chirped device and for a uniform device. High-frequency pulsations are absent in those structures.

In conclusion, we have shown that ultrahigh frequency self-pulsations can be obtained in a single-section DFB laser if the grating is asymmetrically chirped. While most work on high-frequency pulsations in DFB lasers suggest a need for multisection devices, we have shown that these oscillations can occur in a simpler single-section device with the appropriate chirp. Such chirped DFB lasers can be readily made by using the bent waveguide method.[3] For sufficiently high coupling strengths, pulsation frequencies as high as a terahertz may be obtained.

[1] A. Suzuki and K. Tada, Proc. SPIE **239**, 10 (1980).
[2] P. Zhou and G. S. Lee, Appl. Phys. Lett. **56**, 1400 (1990).
[3] H. Hillmer, A. Grabmaier, S. Hansmann, H.-L. Zhu, H. Burkhard, and K. Magari, IEEE J. Sel. Topics Quantum Electron. **1**, 356 (1995).
[4] M. Möhrle, U. Feiste, J. Hörer, R. Molt, and B. Sartorius, IEEE Photonics Technol. Lett. **4**, 976 (1992).
[5] B. Sartorius, M. Möhrle, and U. Feiste, IEEE J. Sel. Topics Quantum Electron. **1**, 535 (1995).
[6] U. Feiste, D. J. As, and A. Ehrhardt, IEEE Photonics Technol. Lett. **6**, 106 (1994).
[7] H. Wenzel, U. Bandelow, H.-J. Wünsche, and J. Rehberg, IEEE J. Quantum Electron. **QE-32**, 69 (1996).
[8] Y. H. Liao and H. G. Winful, Opt. Lett. **21**, 471 (1996).
[9] L. M. Zhang and J. E. Carroll, IEEE J. Quantum Electron. **QE-28**, 604 (1992).
[10] H. Kogelnik and C. V. Shank, J. Appl. Phys. **43**, 2327 (1972).